American Journal of Botany
Botanical Society of America
leading scientists and educators since 1893

RESEARCH ARTICLE

Some (do not) like it hot: shrub growth is hampered by heat and drought at the alpine treeline in recent decades

Loïc Francon[1,6], Christophe Corona[1], Irène Till-Bottraud[1], Bradley Z. Carlson[2], and Markus Stoffel[3,4,5]

Manuscript received 4 October 2019; revision accepted 30 January 2020.

[1] Université Clermont Auvergne, CNRS, GEOLAB, F-63000 Clermont-Ferrand, France

[2] Centre de Recherches sur les Ecosystèmes d'Altitude (CREA), Observatoire du Mont-Blanc, 74400 Chamonix, France

[3] Climate Change Impacts and Risks in the Anthropocene (C-CIA), Institute for Environmental Sciences, University of Geneva, Geneva, Switzerland

[4] Department of Earth Sciences, University of Geneva, Geneva, Switzerland

[5] Department F.-A. Forel for Environmental and Aquatic Sciences, University of Geneva, Geneva, Switzerland

[6] Author for correspondence (e-mail: loic.francon@etu.uca.fr)

Citation: Francon, L., C. Corona, I. Till-Bottraud, B. Z. Carlson, and M. Stoffel. 2020. Some (do not) like it hot: Shrub growth is hampered by heat and drought at the alpine treeline in recent decades. *American Journal of Botany* 107(4): 1–11.

doi:10.1002/ajb2.1459

PREMISE: Mountain ecosystems are particularly sensitive to climate change. However, only a very small number of studies exist so far using annually resolved records of alpine plant growth spanning the past century. Here we aimed to identify the effects of heat waves and drought, driven by global warming, on annual radial growth of *Rhododendron ferrugineum*.

METHODS: We constructed two century-long shrub ring-width chronologies from *R. ferrugineum* individuals on two adjacent, north- and west-facing slopes in the southern French Alps. We analyzed available meteorological data (temperature, precipitation and drought) over the period 1960–2016. Climate–growth relationships were evaluated using bootstrapped correlation functions and structural equation models to identify the effects of rising temperature on shrub growth.

RESULTS: Analysis of meteorological variables during 1960–2016 revealed a shift in the late 1980s when heat waves and drought increased in intensity and frequency. In response to these extreme climate events, shrubs have experienced significant changes in their main limiting factors. Between 1960 and 1988, radial growth on both slopes was strongly controlled by the sum of growing degree days during the snow free period. Between 1989 and 2016, August temperature and drought have emerged as the most important.

CONCLUSIONS: Increasing air temperatures have caused a shift in the growth response of shrubs to climate. The recently observed negative effect of high summer temperature and drought on shrub growth can, however, be buffered by topographic variability, supporting the macro- and microrefugia hypotheses.

KEY WORDS dendrochronology; dendroecology; drought; dwarf shrubs; Ericaceae; heat wave; *Rhododendron ferrugineum*; shrub expansion; standardized precipitation–evaporation index; structural equation model.

Mountain regions are warming at a rate twice as fast as the global average and are thus expected to undergo a greater relative temperature increase over the next century (Stocker et al., 2013; Mountain Research Initiative EDW Working Group, 2015). In the European Alps, recent warming has not been linear, and a sharp increase in annual temperature has emerged in meteorological records since the end of the 1980s (Gobiet et al., 2014; Beniston et al., 2018). A growing body of evidence documents changes in mountain vegetation in response to longer and warmer growing seasons, such as (1) an upward shift in species distribution (Lenoir et al., 2008), (2) increasing biodiversity on summits (Pauli et al., 2012; Steinbauer et al., 2018), (3) phenological shifts (Choler, 2015), (4) increasing plant productivity and long-term greening (Carlson et al., 2017; Filippa et al., 2019), and (5) a reshuffling and thermophilization of alpine communities (Gottfried et al., 2012). However, in sharp contrast to the Arctic, where widespread shrub expansion has been identified (Myers-Smith et al., 2011, 2015a), evidence remains scarce for a similar large-scale shrub expansion in the European Alps, even if some regional studies have documented a denser shrub cover above treeline during recent decades (Anthelme et al., 2007; Cannone et al., 2007; Carlson et al., 2017).

Although alpine and arctic ecosystems both experience short and cold growing seasons, Ernakovich et al. (2014) recently predicted alpine ecosystems to be more drought-sensitive than their arctic counterparts under the influence of climate change. According to the authors, alpine plants will potentially experience earlier senescence as a result of reduced water availability and will thus be unable to extend their growing season, despite earlier snow melt out. At the same time, however, nonlinear responses to rising summer temperatures have been locally observed in dry arctic landscapes, where soil moisture seems to buffer the positive effect of higher temperatures on shrub growth (Myers-Smith et al., 2015a; Ackerman et al., 2017; Bjorkman et al., 2018; Gamm et al., 2018).

In the European Alps, the frequency and intensity of summer heat waves and extreme drought events have increased in recent decades, and this increase is expected to continue with increasing temperatures (Easterling, 2000; Orsenigo et al., 2014; Russo et al., 2014; Corona-Lozada et al., 2019). To date, only a handful of studies have documented responses of alpine ecosystems to heat waves and drought, leading to contrasting results (Jolly et al., 2005; De Boeck et al., 2016; Cremonese et al., 2017; Corona-Lozada et al., 2019). Corona-Lozada et al. (2019), De Boeck et al. (2016), and Cremonese et al. (2017) documented a negative effect of summer drought on alpine plant productivity, which was clearly aggravated by heat waves. In the Swiss Alps, Jolly et al. (2005) reported that the 2003 heat wave would have had positive effects on plant growth above treeline through an extension of the growing season, but negative impacts at lower elevations, where the higher evaporative demand increased drought sensitivity.

Shrub dendroecology, which analyzes radial stem growth over time, allows us to contextualize the response of woody vegetation to climate variability in a longer term context (Myers-Smith et al., 2015b). For this reason, the approach has been used widely across the Arctic biome to assess climatic drivers of shrub expansion. In comparison, only a handful of chronologies have been constructed so far for shrubs in alpine regions (e.g., Liang and Eckstein, 2009; Franklin, 2013; Lu et al., 2015). Dendroecological studies carried out in the European Alps hitherto identified that increasing summer temperatures and earlier snow melt-out dates would have a positive effect on shrub growth (Pellizzari et al., 2014; Francon et al., 2017; Carrer et al., 2019). By contrast, in the Mediterranean mountain ranges of southeastern Spain, juniper shrubs were shown to experience a change in their main limiting factors, shifting from temperature and growing season length to water availability (García-Cervigón et al., 2018). The authors further demonstrated that contrasting microclimates—induced by topography—could modulate the response of junipers to ongoing climate change.

Here, we investigated long-term climate–growth relationships for the widespread and dominant alpine shrub species, *Rhododendron ferrugineum* L. (Ericaceae), using samples within the Queyras massif located in the southern French Alps. We hypothesize that the recent increase in drought and heat waves could counteract the beneficial effects that rising temperatures have on shrub radial growth, but that this buffering could be different and/or modulated according to slope aspect. To test this hypothesis, we (1) identified the main climatic parameters controlling *R. ferrugineum* radial growth at the study site by using a bootstrap correlation analysis, (2) included these parameters in structural equation models (SEM) to disentangle their respective effects on two adjacent slopes of different aspects, and (3) looked for potential shifts in the climatic drivers of shrub growth, resulting from climate changes since the late 1980s.

METHODS

Study site and climate

The study site is located in the upper Guil Valley in the French southern intra-alpine Queyras massif (Fig. 1A–C). Geology of the region is dominated by Mesozoic *schistes lustrés* (Tricart and Lemoine, 1986), a tectonic stack of blue schist to green schist-facies carbonate metasediments on which acidic soils have developed. More precisely, the site is located at treeline (2350 m a.s.l.) and dominated by the Crête des Baysses near the French-Italian border. The site was chosen to minimize effects other than slope aspect (geographical proximity for similar bedrock conditions, climate, and slope inclination). *Rhododendron ferrugineum* individuals were sampled on two adjacent, west-facing (Queyras West [QW], Fig. 1C, D) and north-facing (Queyras North, [QN], Fig. 1C, E) slopes. The landscape is dominated by a *Rhododendron ferrugineum* heathland intermixed with *Vaccinium* sp. and *Salix* sp. shrubs and isolated *Larix decidua* and *Pinus cembra* trees. Slope angles (30°) are comparable on both slopes. Microtopography is very regular at QW but slightly more heterogeneous at QN, which is situated in the catchment area of the Nalbert torrent. Climate is characterized by a mix of montane-Mediterranean and continental influences (Touflan et al., 2010). According to the SAFRAN-Crocus meteorological data (1960–2016), downscaled to the location of our study sites, annual precipitation is 873 mm. Monthly precipitation totals are lowest in winter and summer (P-February = 51 mm, P-July = 58 mm) and largest in spring and autumn (P-June = 84 mm, P-October = 98 mm). July (9.4°C) is the warmest month, and snow cover remains until 24 May (±12 days) at QW and 1 June (±12 days) at QN.

Sample collection and preparation

Rhododendron ferrugineum is a dominant mountain shrub in the siliceous Alps from about 1600 to 2500 m a.s.l. (Ozenda, 1985), where it is often found as the dominant species in subalpine dwarf shrub communities (Pornon and Doche, 1996). It can form large heathlands, colonizing grazed or abandoned grasslands on north-, west-, and northwest-facing slopes of the central and southern Alps (Escaravage et al., 1997). High longevity and clearly identifiable annual rings—discriminated by a band of radially aligned, thick walled latewood fibers, flattened along the ring boundary—make *R. ferrugineum* a promising model to study shrub response to long-term climate variability (Francon et al., 2017).

In this study, a total of 36 randomly selected *R. ferrugineum* individuals were sampled in June 2017 at a minimum distance of 5 m between each other, 18 at QW and 18 at QN. The main stem of each specimen was cut at the level of the root collar. In the lab, two to three cross sections 20 μm thick were prepared for each stem, a first sample at the root collar and further samples at 10–20-cm steps along the stem, so as to apply an approach known as serial-sectioning method (Kolishchuk, 1990). Cross sections were then stained with safranin (1% w/v in 70% v/v ethanol) and astra blue (1% w/v in 100% ethanol), and permanently fixed on microslides with Canada balsam (Schweingruber et al., 2011). High-resolution digital pictures were taken using a Carl Zeiss Axio Observer Z1 coupled to a Zeiss AxioCam MR R3 camera (Zeiss, Jena, Germany) at 40–100× magnification. Individual images were merged automatically to cover entire cross sections using Zen 2011 software (Zeiss, Jena, Germany).

Chronology development

Ring widths were measured along three radii on each section from digital images with CooRecorder 7.6 (CYBIS Elektonik & Data AB, Saltsjöbaden, Sweden). Radial measurements along the chosen radii were supplemented by careful visual inspection of each cross section to eliminate annual growth underestimation caused

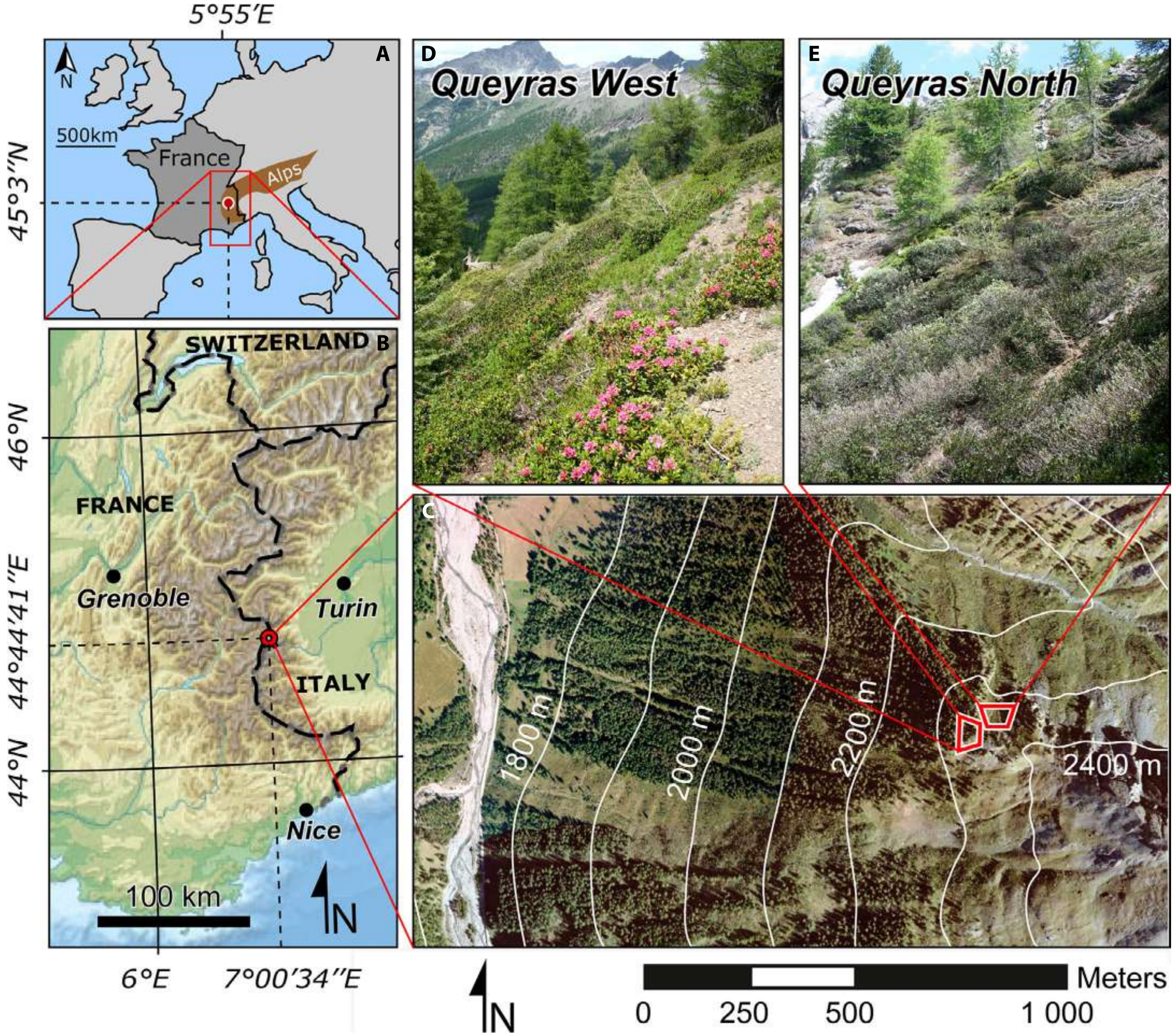

FIGURE 1. (A, B, C) Location and overview of the (D) west-facing (QW: Queyras West) and (E) north-facing slopes (QN: Queyras North) selected for sampling in the Queyras massif (Southern French Alps). Photographs of QW (D) and QN (E) were taken on 15 June 2017.

by partially missing rings. Cross-dating was based on a three-step procedure involving a comparison of growth curves (1) between the three radii measured within a single cross section, (2) among the mean growth curves of all sections within individual plants, and (3) between the mean growth curves of all shrubs on each of the slopes sampled (Francon et al., 2017; Shetti et al., 2018). The output of the visual cross-dating was checked statistically with COFECHA (Holmes, 1994).

After cross-dating, the mean series of each section was standardized (Fritts, 1976; Cook and Kairiukstis, 1990) in ARSTAN (Cook, 1987). To remove age-related growth trends and other possible biological effects, we standardized each growth curve at the section scale using a negative exponential function to obtain detrended chronologies. A negative exponential function was chosen as a rather conservative growth trend model to keep as much climatic signal as possible in the series. Growth indices (referred to as ring-width indices [RWI]) were averaged to mean standard individual and site chronologies, on a year-by-year basis, and by using a bi-weighted robust mean that reduces the influence of outliers (Cook and Peters, 1981). In addition to the standard chronologies, we also computed so-called residual chronologies in which auto-correlation was removed.

Descriptive statistics including standard deviation (SD), mean sensitivity (MS), and autocorrelation (AC) were computed for both detrended chronologies. In addition, the expressed population signal (EPS; Wigley et al., 1984), subsample signal strength (SSS; Wigley et al., 1984; Buras, 2017) and mean inter-series correlation (rbar) were computed using the ARSTAN software to evaluate the robustness of each chronology. The EPS and SSS statistics quantifies the strength of the common climate signal in the tree-ring proxies by calculating how well a finite subsample represents an infinite (EPS) or finite sample (SSS) (Wigley et al., 1984; Buras, 2017). For both SSS and EPS, a threshold of 0.85 was used to guarantee robustness of the chronologies.

Meteorological and climatic data

Monthly temperature, precipitation sums, and snow-related parameters were extracted from the SAFRAN-Crocus reanalysis. The SAFRAN analysis system combines in situ meteorological observations with synoptic-scale meteorological fields to provide continuous time series of meteorological variables at hourly resolution, for elevation bands of 300 m, different slope aspects and angles within spatial units, referred to as "massifs" (Queyras in the case of this study), for which meteorological variables are assumed to be horizontally homogenous (Durand et al., 2009). In addition, the Crocus model was run specifically for QW and QN. The Crocus model provides corresponding reanalysis of snow conditions and underlying ground temperature for the same time span as SAFRAN reanalysis (Durand et al., 2009; Vionnet et al., 2012). Vegetation was represented in a simplified manner in the simulations, assuming grassy conditions to simulate typical snow conditions and underlying ground temperature for open areas. The data set extends back to August 1958.

From the hourly outputs, we extracted (1) monthly temperature and precipitation sums, (2) dates of snow melt-out (defined as the last day when snow cover reached at mean height of the shrub canopy located at ca. 50 cm), (3) snow-free growing degree days (hereafter referred to as SF-GDD and computed as the sum of positive air temperature from the melt-out date to the end of growth period arbitrarily fixed at 31August), and (4) heat wave index (HWI). The HWI series accounting for the magnitude and the duration of heat waves (Russo et al., 2014) was computed from 1 July to 10 September over the 1960–2016 period. First, we computed a daily temperature threshold defined as the 80th percentile of the daily maxima over the period 1959–2016. This threshold was calculated by considering a 30-day window centered on the day of interest. In a second step, we extracted episodes with at least three consecutive days during which the maximum air temperatures exceeded the threshold. These episodes were considered as heat waves. Finally, we summed daily maximum temperatures of each episode to obtain a measure of the magnitude of the heat wave.

We used the standardized precipitation-evapotranspiration index (SPEI) developed by Vicente-Serrano et al. (2010) as a metric to quantify drought. SPEI combined precipitation, temperature, wind, nebulosity, and relative humidity series from the SAFRAN analysis system for the period 1960–2016 at time intervals of 2 (SPEI2) and 12 months (SPEI12, September to August). SPEI2 was used for climate–growth analyses, whereas SPEI12 was employed to identify dry years.

Climate-growth modelling

We used structural equation models (SEMs) to unravel the direct and indirect effects of interrelated climatic variables, in particular heat waves and drought, on *R. ferrugineum* growth. The SEM is an extension of a path analysis and represents a relevant statistical framework to model multivariate effects of driving factors on a response variable (Grace and Bollen, 2005).

As a preliminary analysis to determine the nature of causal relations between climate variables and the shrub ring chronologies implemented in the path diagrams of each structural equation model, we computed correlations between the standard and residual chronologies and monthly climatic variables using bootstrapped correlation functions (BCF) using the Treeclim package (Zang and Biondi, 2015) in R (R Core Team, 2016). The climatic data set included monthly temperature, precipitation sums, snow melt-out timing, SF-GDD, and SPEI2 sequences. For each variable, we included values from July of the year preceding growth-ring formation ($n - 1$) to September of the year of actual ring formation (n), thereby analyzing a set of 51 predictors. The relationship between the HWI and the shrub-ring chronologies was evaluated using Spearman's rank correlation. Significance was assessed at $p < 0.05$ through a 1000 bootstrap replicate approach.

Based on this pre-selection of variables and to unravel the potential impacts of rising temperatures on shrub growth, we computed SEMs for two distinct periods: 1960–1988 and 1989–2016. The splitting of the record in two subsets of equal length was motivated by the fact that the meteorological series, especially HWI, indicated a threshold around 1989. In addition, statistically significant differences were observed in mean summer temperature, SPEI12 and HWI between both subperiods as shown in Appendix S1 (also see the Results section). In the resulting models, the set of causal assumptions are represented as arrows on diagrams, and the values of standardized path coefficients quantify the relative impact of a driving variable on a response variable (Jonas et al., 2008). Before the analyses, we verified that the diagrams did not include any feedbacks and that relationships among variables could be described using linear models. We checked the data for goodness-of-fit by using the χ^2 statistic with a $p > 0.05$ cut-off (Grace, 2006) and the comparative fit index (CFI > 0.90, Bentler, 1990). To perform and control SEMs, we used the Lavaan package (Rosseel, 2012) in R. Akaike information criterion (AIC) was used to compare performance among competing SEMs.

RESULTS

Evolution of summer climate in the Queyras massif

Figure 2 is a synthesis of the evolution of summer conditions in the Queyras massif with a specific focus on dry conditions and heat waves. The linear regressions show significant increasing trends ($P < 0.001$) for mean summer (June–August) temperature during 1960–2016. For the same period, we observed a significant decrease in the annual SPEI computed from September of the previous ($n - 1$) to August of the current (n) year ($P < 0.001$), pointing to an increasing frequency of years with water deficit. Mean values of SPEI12 thereby decreased from 0.41 to −0.41 for the subperiods 1960–1988 and 1989–2016, respectively. At the same time, mean summer (June–August) temperatures increased from 7.9°C to 9.2°C. In addition, HWI values revealed an increase in the frequency of extremely warm summers since 1989 (see Appendix S1). The two strongest heat waves in the record occurred during the summers 2003 and 2015. They were of comparable magnitude with a HWI of 138.5 and 139.4, respectively. Very warm summers were also recorded in 2016 (HWI = 123.2) and 2012 (HWI = 104.8). However, no significant trend was observed in the summer rainfall series over the same period.

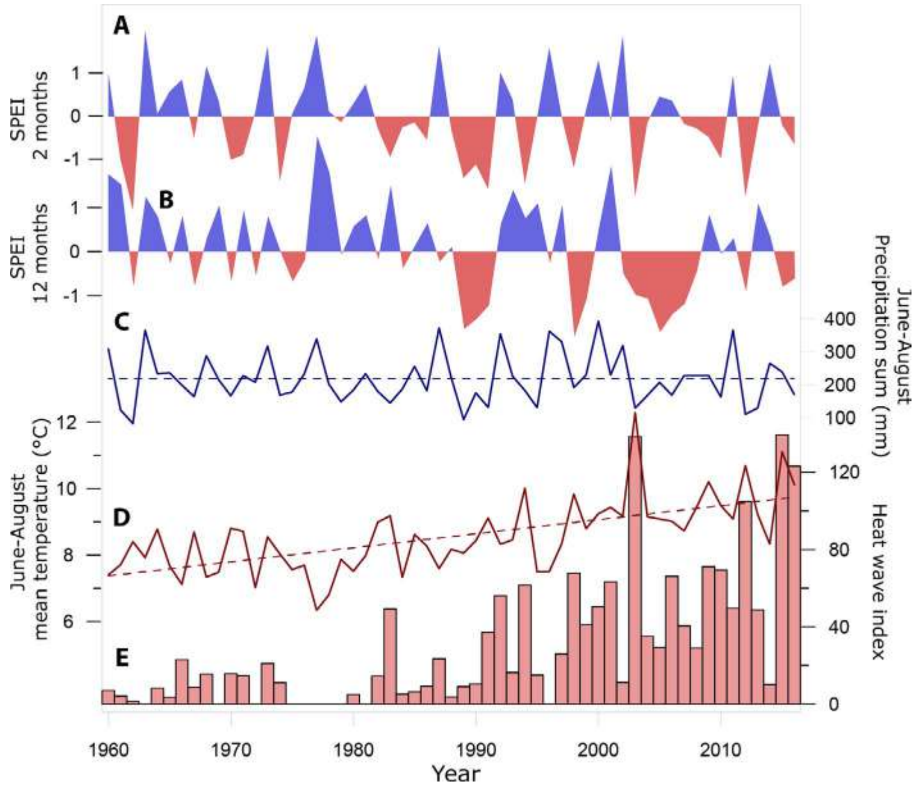

FIGURE 2. Synthesis of climate evolution during summers in the Queyras massif for 1959–2016, with a specific focus on dry conditions and heat waves. (A, B) Evolution of the 2-month (i.e., July and August) and 12-month (September–August) standardized precipitation–evapotranspiration index (SPEI). Negative SPEI values correspond to dry conditions. The evolution of (C) summer (June–August) precipitation sums are indicated with a blue line, (D) summer (June–August) mean temperature is shown with a red line. (E) Unscaled values of the heat wave index for 1959–2016. The dotted blue and red lines indicate linear trends for summer precipitation sums and mean temperatures, respectively.

Statistics of the chronologies

Cross-dating was successful for 10 individuals at QN and 14 individuals at QW (Fig. 3, Table 1). On average, shrubs at QN were significantly older (mean age: 83 years) than at QW (50 years). Annual radial increment between cambial ages at 20 and 39 years was, on average, 0.09 mm at QN and significantly higher at QW (0.14 mm, $P < 0.001$). The rbar values computed between the detrended ring width series were 0.42 and 0.56 for QN and QW, respectively. EPS values of 0.89 at QN and 0.93 at QW attest to the strong coherence of growth between individuals selected within both chronologies. Noteworthy, the SSS (and EPS computed for 30-year moving periods) values exceeded the 0.85 threshold from 1949 (1959) at QW and from 1938 (1952) onward at QN. Autocorrelation (0.13 at QW and 0.22 at QN) was limited at both sampling sites. Mean sensitivity at QN (MS = 0.33) was slightly higher than at QW (MS = 0.30).

Climate–growth relationships

Bootstrapped correlation functions (BCFs, Fig. 4) showed significant positive correlations between RWI and SPEI2 for July and August at QW ($r = 0.41$, $P < 0.01$), whereas no significant relationship was found at QN. At QW, shrub ring width was inversely correlated with August temperature (N) ($r = -0.29$, $P < 0.01$) and positively associated with summer (July–August) precipitation sum ($r = 0.30$, $P < 0.01$). At QN, we found positive relationships of RWI with October ($N - 1$, $r = 0.20$, $P < 0.05$) and July (N, $r = 0.22$, $P < 0.05$) mean temperatures. Radial growth was negatively correlated with precipitation sums in October ($N - 1$, $r = -0.26$, $P < 0.05$), but no significant correlation could be found with respect to precipitation sums during the growing season. The Spearman correlation between the heat wave index and RWI was negative and stronger at QW than at QN, but again not significant at either of the slopes ($\rho = -0.26$, P = 0.06 and $\rho = -0.04$, $P = 0.76$ at QW and QN, respectively). The four heat waves of 2003, 2012, 2015, and 2016 were systematically associated with ring widths that were smaller than average at QW (RWI = 0.836, 0.727, 0.784, and 0.964, in chronological order) and with average or small rings at QN (RWI = 1.072, 0.800, 0.899, and 0.743, in chronological order). With regard to winter conditions, RWI was significantly limited by above-average precipitation sums at QN ($r = -0.34$, $P < 0.01$) and by snow melt-out dates ($r = -0.27$, $P < 0.05$) at QW.

Based on these initial results, we hypothesized that shrub growth would depend on SF-GDD which in turn depended on melt-out dates and, thus, possibly mitigated by the negative effects of drought (Fig. 5). The SEMs computed over the period 1960–2016 explain 24% and 14% of inter-annual variations in ring width of *R. ferrugineum* at QW and QN, respectively, and present a good performance ($\chi^2 = 14.87$, df = 15, $P = 0.47$, CFI = 1.00 at QW and $\chi^2 = 19.2$, df = 14, $P = 0.16$, CFI = 0.98 at QN). Modelling results confirm that SF-GDD is a strong driver of radial growth at QN (path coefficient of 0.40, $P < 0.05$) and to a lesser extent at QW (0.29, $P < 0.1$). At both sites, SF-GDD are controlled by snow-free period temperatures and melt-out dates which in turn will depend significantly on December–March precipitation sums and on spring temperature (April temperature at QW and May temperature at QN).

The SEMs support the hypothesis of SPEI2 having a significant effect on RWI at QW with a path coefficient of 0.34 ($P < 0.01$), whereas no such effect was detected between SPEI (July + August) and RWI at QN. August mean temperature had a negative effect on RWI at QW (-0.32, $P < 0.05$) and at QN (-0.42, $P < 0.01$). The SEM computed for QW indicates that the latter parameter, in combination with summer precipitation sums, would also have an indirect effect on radial growth as it controls SPEI2. The inclusion of July (N) as well as October ($N - 1$) temperatures and precipitation sums—parameters that were shown to be significantly correlated to *R. ferrugineum* growth according to BCFs—did not improve the robustness of our SEMs significantly (Appendix S2). Therefore, we present here only the best-performing path model at each site. The SEMs based on the residual chronologies provide comparable results (Appendix S3).

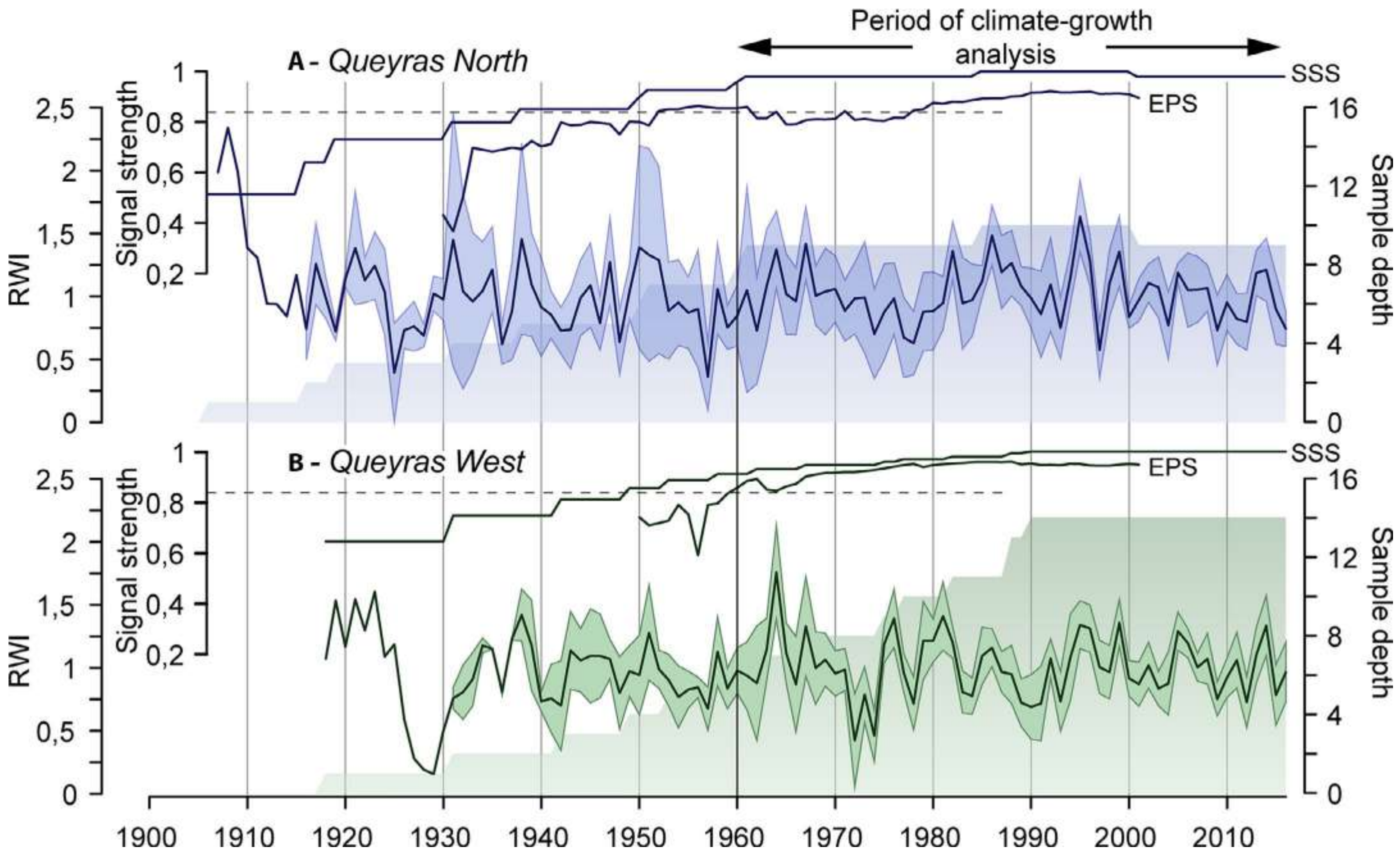

FIGURE 3. Detrended *Rhododendron ferrugineum* ring-width chronologies and the subsample signal strength (SSS) from Queyras North (panel A) and Queyras West (panel B) with their confidence intervals (± 1 SD). The expressed population signal (EPS) is computed with a 30-year moving window (solid line above the chronologies). The horizontal dotted black lines denote the 0.85 signal strength threshold. The vertical continuous line indicates 1960, the starting year for climate–growth analyses. Colored background surfaces represent sample depth.

TABLE 1. Characteristics of *Rhododendron ferrugineum* ring-width chronologies: length, mean age, median ring width computed for raw chronologies and standard deviation (SD), signal strength (rbar and EPS for 1960–2016), mean sensitivity (MS) and first order autocorrelation (AC) (calculated over the entire periods covered by the chronologies. Values refer to series after detrending.

Chronology	First year	Last Year	Mean age	SD	rbar	EPS	MS	AC
QN	1906	2016	83	0.30	0.42	0.89	0.33	0.24
QNres	1906	2016	83	0.21	0.42	0.89	0.28	NA
QW	1918	2016	50	0.27	0.56	0.93	0.30	0.13
QWres	1918	2016	50	0.23	0.56	0.93	0.26	NA

Stationarity of shrub growth–climate relationships over time

The SEMs computed for 1960–1988 and 1989–2016 all displayed p-values for the χ^2 test exceeding 0.05 and CFI values above the 0.9 cut-off. Between 1960 and 1988, the SEMs were comparable and confirmed the crucial impact of SF-GDD on RWI at both sites (0.52 and 0.70, $P < 0.01$ and $P < 0.001$ at QW and QN, respectively). Correlations between August temperatures and radial growth were not significant. A limited effect of SPEI2 is detected at QW (0.31, $P < 0.1$). The SEM computed for the QN ring-width chronology had greater explanatory power ($r^2 = 0.41$) than the one computed for QW chronology ($r^2 = 0.29$).

After 1989, the overall impact of SF-GDD on RWI strongly decreased and are no longer significant at the investigated slopes. At the same time, the path coefficients between August temperature and radial growth decreased from −0.15 to −0.45 ($P < 0.05$) at QW and −0.16 to −0.56 ($P < 0.05$) at QN. Similarly, the influence of SPEI increased at QW (0.38, $P < 0.05$).

DISCUSSION

Shrub dendroecology entails challenging cross-dating due to the often thin, wedging or missing rings (Hollesen et al., 2015; Myers-Smith et al., 2015b), which renders assigning growth rings to an exact year of formation sometimes difficult. Despite these challenges, we were able to build two long-term chronologies in this paper. The north (QN) and west (QW) chronologies presented here are well replicated ($n > 6$) and robust (EPS > 0.85) over the period covered by the meteorological data (i.e., 1960–2016). The rejection rate (33%: 4 of 18 and 8 of 18 individuals at QW and QN, respectively) is mainly related to the occurrence of sequences with extremely

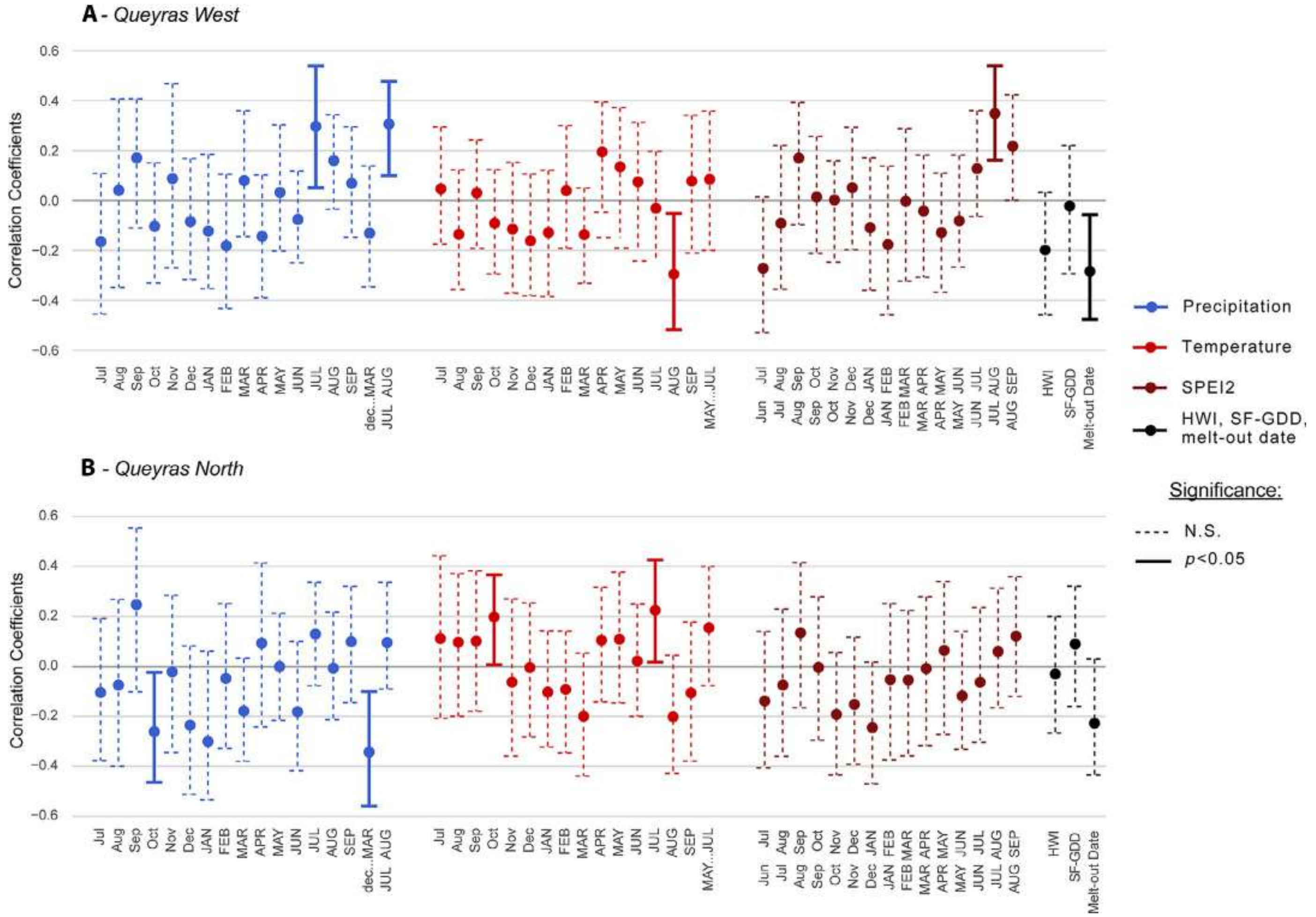

FIGURE 4. Bootstrapped correlations computed between *Rhododendron ferrugineum* detrended chronologies (A, Queyras West; B, Queyras North) and monthly (seasonal) precipitation sums, mean temperatures, 2-month (July–August) standardized precipitation–evapotranspiration index (SPEI2), heat wave index (HWI), snow-free growing degree days (SF-GDD) and snow melt-out dates for 1960–2016. Months of the year preceding (*N* – 1) ring formation (*N*) are shown with lowercase letters; current (*N*) year periods are shown with capital letters.

narrow, wedging or missing rings, difficult to detect and measure. The occurrence of complex samples was larger at QN than at QW.

On average, *R. ferrugineum* ring widths were significantly (33%) thinner at QN than at QW for cambial ages between 20 and 39 years. Similarly, the correlation between both growth-ring chronologies was rather limited ($r = 0.57$ for the period 1960–2016), despite the fact that sampling sites were located next to each other. Differences in shrub productivity and asynchronous signals at both sites are likely related to differences in aspect which have been shown to induce different exposition to photosynthetically active radiation, wind, and snow accumulation (Körner, 2003). These differences are likely leading to colder temperatures and shorter growing seasons at QN. Significantly higher inter-series correlations (rbar) on the west-facing slope also suggest (Dearborn and Danby, 2018) that growth patterns at QW would be more governed by broad-scale climatic patterns influencing growth of all individuals. At QN, by contrast, we hypothesize that microtopography may induce substantial spatial variability in shrub growth as previously observed in topographically complex regions (Danby and Hik, 2007; Leonelli et al., 2009; Ropars et al., 2015; Young et al., 2016; Dearborn and Danby, 2018).

Despite these differences, the bootstrapped correlation functions (BCFs) profiles and structural equation models (SEMs) computed for both slopes show comparable results for 1960–2016. They demonstrate that SF-GDD, which is largely determined by snow melt-out dates, constitutes a strong limiting factor for *R. ferrugineum* radial growth in both topoclimatic contexts. A similar positive effect of increased growing season length and/or temperature has been found at many northern and high-elevation locations worldwide (Forbes et al., 2010; Blok et al., 2011; Pellizzari et al., 2014; Myers-Smith et al., 2015a), where plant growth is temperature limited (Körner, 2003; Wipf, 2010; Wheeler et al., 2016). The negative correlations between radial growth, melt-out timing and winter snowfalls observed in the BCF profiles at QW and QN are congruent with other dendroecological studies carried out in the Alps (Pellizzari et al., 2014; Francon et al., 2017; Carrer et al., 2019). Our results differ from most Arctic studies, however, where the positive effect of snowpack on shrub growth (Zalatan and Gajewski, 2006; Hallinger et al., 2010; Hollesen et al., 2015; Ropars et al., 2015) has been attributed to its thermal insulation effect (Chapin et al., 2005; Sturm et al., 2005; Hallinger et al., 2010). In the Queyras massif, the SEMs revealed that the relationship between winter precipitation and *R. ferrugineum* radial growth is not direct but

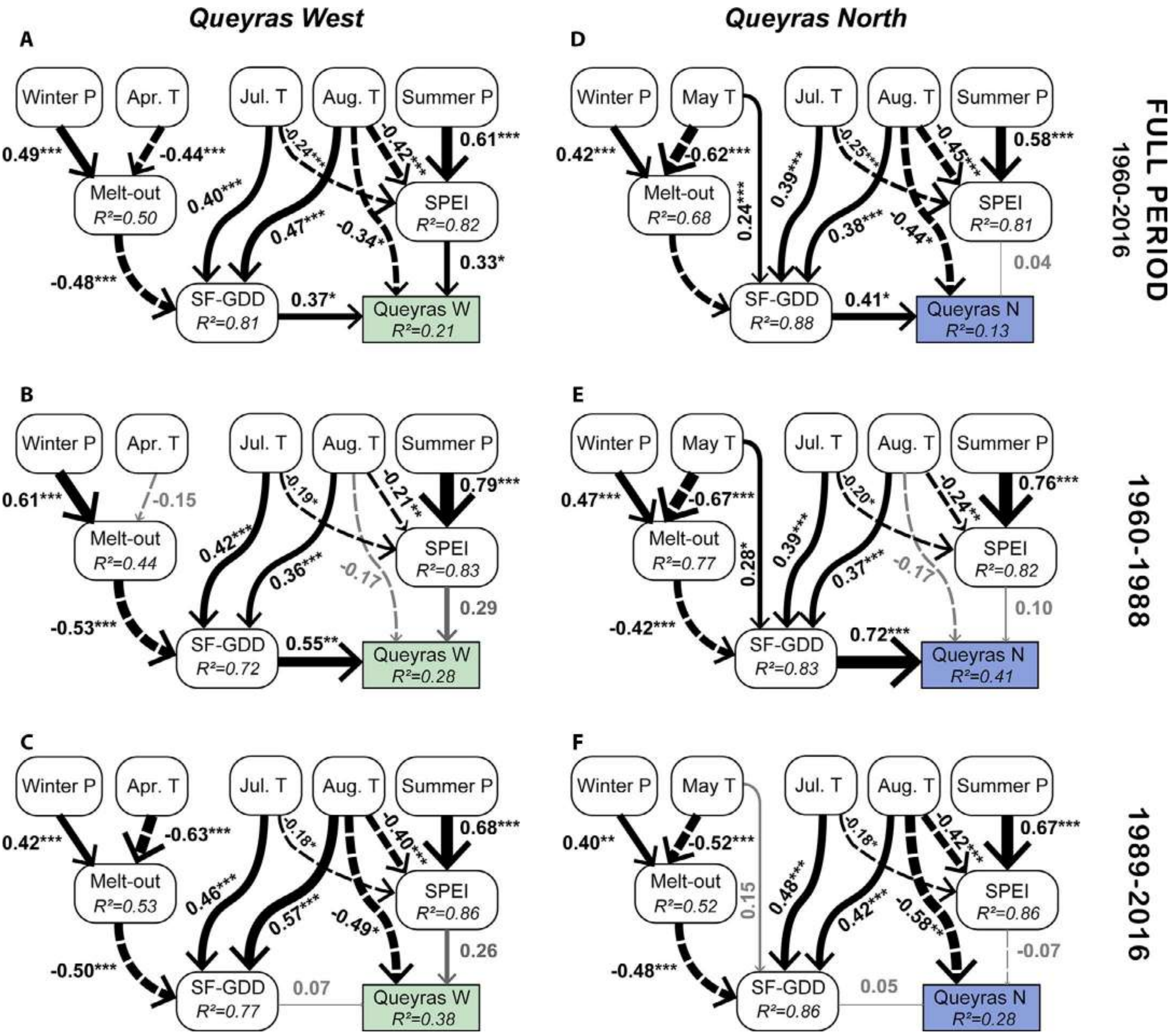

FIGURE 5. Structural equation models (SEMs) showing all climatic variables expected to have a direct or indirect influence on shrub growth and their respective effects on shrub ring-width indices for the Queyras West (left panel, A–C) and Queyras North (right panel, D–F) sites between 1960 and 2016 (A, D), and for subperiods 1960–1988 (B, E) and 1989–2016 (C, F). Black solid arrows denote positive while dotted arrows represent negative significant relationships ($P < 0.05$) between variables. Gray arrows indicate nonsignificant relationships ($P > 0.05$). The thickness of arrows is proportional to the standardized path coefficient. Multiple R^2 values are given in the box of each response variable. ***$P < 0.001$, **$P < 0.01$, *$P < 0.05$, $P < 0.1$ indicate the significance level of each effect.

instead affects available SF-GDD totals by regulating snow cover accumulation and duration.

Analysis of the meteorological series shows (1) an increase in summer temperatures between 1960 and 2016 and (2) stronger annual water deficits and (3) more frequent and severe heat waves since the early 1990s. These changes apparently led to a clear shift in the climate–growth relationships since the late 1980s. In that sense, we observed that *R. ferrugineum* radial growth was controlled mainly by SF-GDD (with the latter depending on snowpack duration) until 1989, but has ever since been limited by August temperatures at both sites and by summer drought at QW. Comparable shifts have been reported in the Mediterranean mountains and at a dry Arctic tundra site. It was shown that junipers from southeastern Spain exhibit a strong drought signal as a response to increasing evapotranspiration rates (García-Cervigón et al., 2018), whereas in Greenland, the growth decline of dwarf birch coincides with a shift in the correlations between growing season air temperatures and neutral to strongly negative plant growth rates (Gamm et al., 2018). Noteworthy, responses to August temperatures comparable to those observed in the Queyras massif since 1989, have remained exceptional and hitherto only observed in the dry environments of the Tibetan plateau (Liang et al., 2012), Mediterranean mountains

(García-Cervigón et al., 2018), or dry arctic tundra (Gamm et al., 2018). In the western Italian Alps, by contrast, Carrer et al. (2019) described a positive association between dwarf juniper growth and summer precipitation but did not report any significant effect of summer temperature on ring width.

Moreover, a negative effect of summer drought on RWI was only observed at QW over the full period considered (1960–2016). Accordingly, on west-facing slopes exposed to higher solar radiation and to earlier snowmelt (Dobrowski, 2011; Carlson et al., 2013), it is highly probable that individual *R. ferrugineum* plants may have experienced higher evaporative demand, especially in recent decades. Similar microsite differences were reported in the Central Norwegian Scandes (Bär et al., 2008), where extremely warm days were demonstrated to limit ring-width development on south-facing slopes, whereas shrubs located on ridges and north-facing slopes still benefited from the higher temperatures. In addition, it seems plausible that the slightly thinner soils at QW could favor competition between roots and thereby exacerbate the sensitivity of individual plants to drought (Pichler and Oberhuber, 2007). Similarly, the potentially larger crowns of growing individuals in recent decades might have increased drought sensitivity. Evergreen shrubs and larger growth forms have, indeed, been demonstrated to be more sensitive to moisture availability than other functional groups (Livensperger et al., 2016; Corona-Lozada et al., 2019). In any case, the limited sensitivity to drought observed at QN is consistent with numerous studies demonstrating that topography can buffer habitat and diversity loss in heterogeneous high mountain landscapes (Scherrer and Körner, 2011; Steinbauer et al., 2018) by providing topoclimatic microrefugia (Patsiou et al., 2014). We may thus hypothesize that shrub populations that are less exposed to solar radiation could be favored in the future (Bär et al., 2008).

We found no clear relationship between heat wave magnitude and shrub radial growth, which may be explained by the fact that extreme events occurred only four times between 1960 and 2016. During these 4 years, *R. ferrugineum* formed thinner than average growth rings at QW and QN, except for summer 2003 when growth was not unusual at QN. Isolating the effects of summer heat waves has proven to be difficult because negative effects of heat stress on mountain plant growth and productivity have only been observed in combination with water deficit (Jolly et al., 2005; De Boeck et al., 2016; Cremonese et al., 2017; Corona-Lozada et al., 2019). A higher correlation between shrub growth at QW and the heat wave index (as compared to QN) is in line with these results.

CONCLUSIONS

For our study site in the southern French Alps, we found that recent increases in summer temperatures, combined with more frequent and intense drought and heat waves, have led to a shift in climatic drivers controlling the growth of *R. ferrugineum*. Whereas radial growth was controlled mainly by growing season length between 1959 and 1988, growth in more recent years has become more sensitive to drought, notably on west-facing slopes exposed to higher solar radiation and earlier snowmelt. The shift reported here still differs quite strongly from trends described in a majority of dendroecological studies for arctic and alpine environments documenting positive effects of increasing air temperature on shrub growth and productivity (Myers-Smith et al., 2015a). Accordingly, at least in the relatively dry context of the southern interior French Alps, our findings support the hypothesis of Ernakovich et al. (2014) who stated that the beneficial aspect of longer and warmer growing seasons on plant productivity may be locally outweighed by the detrimental effect of reduced soil water availability due to higher evaporative demands. This shift in climatic sensitivity may add to the warning signals outlined by Ernakovich et al. (2014) and their prediction of likely future changes in plant community structures in alpine ecosystems. In addition, the limited drought sensitivity observed on the northern slope studied here tends to confirm that micro-topography could mitigate the impact of climate change by providing climate refugia (Patsiou et al., 2014), suggesting that shrub populations that are less exposed to solar radiation, could be favored in the future.

ACKNOWLEDGMENTS

We thank all who contributed to the meteorological series data used in the analyses, especially Carlo Maria Carmagnola and Samuel Morin (Météo-France - CNRS, CNRM, CEN). We are particularly grateful to Brigitte Girard (INRA, PIAF) for her much appreciated help during the tedious laboratory phase. We acknowledge Olivier Voldoire (GEOLAB, CNRS) for technical support. Rhododendron shrubs were sampled with the help of Sébastien Guillet. We also thank the two anonymous reviewers for their careful revisions and suggestions to improve this paper.

AUTHOR CONTRIBUTIONS

All authors contributed to study design and manuscript preparation. L.F. analyzed the data. L.F., C.C., M.S., and B.C. wrote the paper with significant inputs of I.T.B.

DATA AVAILABILITY

All codes and data are available upon request.

SUPPORTING INFORMATION

Additional Supporting Information may be found online in the supporting information tab for this article.

APPENDIX S1. Comparison between 1960–1988 and 1989–2016 mean summer precipitation and temperature (PJJA and TJJA), mean drought index computed for July–August and September (year $n - 1$) to August (year n) (spei2 and spei12, respectively), and median heat wave index (HWI) at our study site. The significance of the differences between the climate series of both time periods (1960–1988 and 1989–2016) was tested using a *t*-test, except for HWI (Mann–Whitney test); $^{***}P < 0.001$, $^{**}P < 0.01$, $^{*}P < 0.05$.

APPENDIX S2. Summary of model selection using the Akaike information criterion (AIC). ΔAIC is the difference in AIC between the best and alternative models.

APPENDIX S3. Structural equation models (SEMs) computed with residual chronologies.

LITERATURE CITED

Ackerman, D., D. Griffin, S. E. Hobbie, and J. C. Finlay. 2017. Arctic shrub growth trajectories differ across soil moisture levels. *Global Change Biology* 23: 4294–4302.

Anthelme, F., J.-C. Villaret, and J.-J. Brun. 2007. Shrub encroachment in the Alps gives rise to the convergence of sub-alpine communities on a regional scale. *Journal of Vegetation Science* 18: 355–362.

Bär, A., R. Pape, A. Bräuning, and J. Löffler. 2008. Growth-ring variations of dwarf shrubs reflect regional climate signals in alpine environments rather than topoclimatic differences. *Journal of Biogeography* 35: 625–636.

Beniston, M., D. Farinotti, M. Stoffel, L. M. Andreassen, E. Coppola, N. Eckert, A. Fantini, et al. 2018. The European mountain cryosphere: a review of its current state, trends, and future challenges. *Cryosphere* 12: 759–794.

Bentler, P. 1990. Comparative fit indexes in structural models. *Psychological Bulletin* 107: 228–246.

Bjorkman, A. D., I. H. Myers-Smith, S. C. Elmendorf, S. Normand, N. Rüger, P. S. A. Beck, A. Blach-Overgaard, et al. 2018. Plant functional trait change across a warming tundra biome. *Nature* 562: 57–62.

Blok, D., U. Sass-Klaassen, G. Schaepman-Strub, M. M. P. D. Heijmans, P. Sauren, and F. Berendse. 2011. What are the main climate drivers for shrub growth in Northeastern Siberian tundra? *Biogeosciences* 8: 1169–1179.

Buras, A. 2017. A comment on the expressed population signal. *Dendrochronologia* 44: 130–132.

Cannone, N., S. Sgorbati, and M. Guglielmin. 2007. Unexpected impacts of climate change on alpine vegetation. *Frontiers in Ecology and the Environment* 5: 360–364.

Carlson, B. Z., C. F. Randin, I. Boulangeat, S. Lavergne, W. Thuiller, and P. Choler. 2013. Working toward integrated models of alpine plant distribution. *Alpine Botany* 123: 41–53.

Carlson, B. Z., M. C. Corona, C. Dentant, R. Bonet, W. Thuiller, and P. Choler. 2017. Observed long-term greening of alpine vegetation—a case study in the French Alps. *Environmental Research Letters* 12: 114006.

Carrer, M., E. Pellizzari, A. L. Prendin, M. Pividori, and M. Brunetti. 2019. Winter precipitation—not summer temperature—is still the main driver for alpine shrub growth. *Science of the Total Environment* 682: 171–179.

Chapin F. S. III, M. Sturm, M. C. Serreze, J. P. McFadden, J. R. Key, A. H. Lloyd, A. D. McGuire, et al. 2005. Role of land-surface changes in Arctic summer warming. *Science* 310: 657–660.

Choler, P. 2015. Growth response of temperate mountain grasslands to interannual variations in snow cover duration. *Biogeosciences* 12: 3885–3897.

Cook, E. R. 1987. The decomposition of tree-ring series for environmental studies. *Tree Ring Bulletin* 47: 37–59.

Cook, E. R., and L. A. Kairiukstis [eds.]. 1990. Methods of dendrochronology. Springer, Dordrecht, Netherlands.

Cook, E. R., and K. Peters. 1981. The smoothing spline: a new approach to standardizing forest interior tree-ring width series for dendroclimatic studies. *Tree Ring Bulletin* 41: 45–53.

Corona-Lozada, M. C., S. Morin, and P. Choler. 2019. Drought offsets the positive effect of summer heat waves on the canopy greenness of mountain grasslands. *Agricultural and Forest Meteorology* 276–277: 107617.

Cremonese, E., G. Filippa, M. Galvagno, C. Siniscalco, L. Oddi, U. Morra di Cella, and M. Migliavacca. 2017. Heat wave hinders green wave: the impact of climate extreme on the phenology of a mountain grassland. *Agricultural and Forest Meteorology* 247: 320–330.

Danby, R. K., and D. S. Hik. 2007. Variability, contingency and rapid change in recent subarctic alpine tree line dynamics. *Journal of Ecology* 95: 352–363.

De Boeck, H. J., S. Bassin, M. Verlinden, M. Zeiter, and E. Hiltbrunner. 2016. Simulated heat waves affected alpine grassland only in combination with drought. *New Phytologist* 209: 531–541.

Dearborn, K. D., and R. K. Danby. 2018. Topographic influences on ring widths of trees and shrubs across alpine treelines in southwest Yukon. *Arctic, Antarctic, and Alpine Research* 50: e1495445.

Dobrowski, S. Z. 2011. A climatic basis for microrefugia: the influence of terrain on climate: a climatic basis for microrefugia. *Global Change Biology* 17: 1022–1035.

Durand, Y., G. Giraud, M. Laternser, P. Etchevers, L. Mérindol, and B. Lesaffre. 2009. Reanalysis of 47 years of climate in the French Alps (1958–2005): climatology and trends for snow cover. *Journal of Applied Meteorology and Climatology* 48: 2487–2512.

Easterling, D. R. 2000. Climate extremes: observations, modeling, and impacts. *Science* 289: 2068–2074.

Ernakovich, J. G., K. A. Hopping, A. B. Berdanier, R. T. Simpson, E. J. Kachergis, H. Steltzer, and M. D. Wallenstein. 2014. Predicted responses of arctic and alpine ecosystems to altered seasonality under climate change. *Global Change Biology* 20: 3256–3269.

Escaravage, N., A. Pornon, B. Doche, and I. Till-Bottraud. 1997. Breeding system in an alpine species: *Rhododendron ferrugineum* L. (Ericaceae) in the French northern Alps. *Canadian Journal of Botany* 75: 736–743.

Filippa, G., E. Cremonese, M. Galvagno, M. Isabellon, A. Bayle, P. Choler, B. Z. Carlson, et al. 2019. Climatic drivers of greening trends in the Alps. *Remote Sensing* 11: 2527.

Forbes, B. C., M. M. Fauria, and P. Zetterberg. 2010. Russian Arctic warming and 'greening' are closely tracked by tundra shrub willows. *Global Change Biology* 16: 1542–1554.

Francon, L., C. Corona, E. Roussel, J. Lopez Saez, and M. Stoffel. 2017. Warm summers and moderate winter precipitation boost *Rhododendron ferrugineum* L. growth in the Taillefer massif (French Alps). *Science of the Total Environment* 586: 1020–1031.

Franklin, R. S. 2013. Growth response of the alpine shrub, *Linanthus pungens*, to snowpack and temperature at a rock glacier site in the eastern Sierra Nevada of California, USA. *Quaternary International* 310: 20–33.

Fritts, H. C. 1976. Tree rings and climate. Academic Press, London, UK.

Gamm, C. M., P. F. Sullivan, A. Buchwal, R. J. Dial, A. B. Young, D. A. Watts, S. M. P. Cahoon, et al. 2018. Declining growth of deciduous shrubs in the warming climate of continental western Greenland. *Journal of Ecology* 106: 640–654.

García-Cervigón, A. I., J. C. Linares, M. García-Hidalgo, J. J. Camarero, and J. M. Olano. 2018. Growth delay by winter precipitation could hinder *Juniperus sabina* persistence under increasing summer drought. *Dendrochronologia* 51: 22–31.

Gobiet, A., S. Kotlarski, M. Beniston, G. Heinrich, J. Rajczak, and M. Stoffel. 2014. 21st century climate change in the European Alps—a review. *Science of the Total Environment* 493: 1138–1151.

Gottfried, M., H. Pauli, A. Futschik, M. Akhalkatsi, P. Barančok, J. L. Benito Alonso, G. Coldea, et al. 2012. Continent-wide response of mountain vegetation to climate change. *Nature Climate Change* 2: 111–115.

Grace, J. B. 2006. Structural equation modeling and natural systems. Cambridge University Press, Cambridge, UK.

Grace, J. B., and K. A. Bollen. 2005. Interpreting the results from multiple regression and structural equation models. *Bulletin of the Ecological Society of America* 86: 283–295.

Hallinger, M., M. Manthey, and M. Wilmking. 2010. Establishing a missing link: warm summers and winter snow cover promote shrub expansion into alpine tundra in Scandinavia. *New Phytologist* 186: 890–899.

Hollesen, J., A. Buchwal, G. Rachlewicz, B. U. Hansen, M. O. Hansen, O. Stecher, and B. Elberling. 2015. Winter warming as an important co-driver for *Betula nana* growth in western Greenland during the past century. *Global Change Biology* 21: 2410–2423.

Holmes, R. L. 1994. Dendrochronology program library user's manual. Laboratory of Tree-Ring Research, University of Arizona, Tucson, AZ, USA.

Jolly, W. M., M. Dobbertin, N. E. Zimmermann, and M. Reichstein. 2005. Divergent vegetation growth responses to the 2003 heat wave in the Swiss Alps: vegetation response to alpine heat wave. *Geophysical Research Letters* 32: 1–4.

Jonas, T., C. Rixen, M. Sturm, and V. Stoeckli. 2008. How alpine plant growth is linked to snow cover and climate variability. *Journal of Geophysical Research* 113.

Kolishchuk, V. 1990. Dendroclimatological study of prostrate woody plant. Methods of dendrochronology, applications in the environmental sciences, 51–55. Springer, Dordrecht, Netherlands.

Körner, C. 2003. Alpine plant life: functional plant ecology of high mountain ecosystems, 2nd ed. Springer, Berlin, Germany.

Lenoir, J., J. C. Gegout, P. A. Marquet, P. de Ruffray, and H. Brisse. 2008. A Significant upward shift in plant species optimum elevation during the 20th century. *Science* 320: 1768–1771.

Leonelli, G., M. Pelfini, G. Battipaglia, and P. Cherubini. 2009. Site-aspect influence on climate sensitivity over time of a high-altitude *Pinus cembra* tree-ring network. *Climatic Change* 96: 185–201.

Liang, E., and D. Eckstein. 2009. Dendrochronological potential of the alpine shrub *Rhododendron nivale* on the south-eastern Tibetan Plateau. *Annals of Botany* 104: 665–670.

Liang, E., X. Lu, P. Ren, X. Li, L. Zhu, and D. Eckstein. 2012. Annual increments of juniper dwarf shrubs above the tree line on the central Tibetan Plateau: a useful climatic proxy. *Annals of Botany* 109: 721–728.

Livensperger, C., H. Steltzer, A. Darrouzet-Nardi, P. F. Sullivan, M. Wallenstein, and M. N. Weintraub. 2016. Earlier snowmelt and warming lead to earlier but not necessarily more plant growth. *AoB Plants* 8: plw021.

Lu, X., J. J. Camarero, Y. Wang, E. Liang, and D. Eckstein. 2015. Up to 400-year-old *Rhododendron* shrubs on the southeastern Tibetan Plateau: prospects for shrub-based dendrochronology. *Boreas* 44: 760–768.

Mountain Research Initiative EDW Working Group. 2015. Elevation-dependent warming in mountain regions of the world. *Nature Climate Change* 5: 424–430.

Myers-Smith, I. H., B. C. Forbes, M. Wilmking, M. Hallinger, T. Lantz, D. Blok, K. D. Tape, et al. 2011. Shrub expansion in tundra ecosystems: dynamics, impacts and research priorities. *Environmental Research Letters* 6: 045509.

Myers-Smith, I. H., S. C. Elmendorf, P. S. A. Beck, M. Wilmking, M. Hallinger, D. Blok, K. D. Tape, et al. 2015a. Climate sensitivity of shrub growth across the tundra biome. *Nature Climate Change* 5: 887–891.

Myers-Smith, I. H., M. Hallinger, D. Blok, U. Sass-Klaassen, S. A. Rayback, S. Weijers, A. J. Trant, et al. 2015b. Methods for measuring arctic and alpine shrub growth: a review. *Earth-Science Reviews* 140: 1–13.

Orsenigo, S., A. Mondoni, G. Rossi, and T. Abeli. 2014. Some like it hot and some like it cold, but not too much: plant responses to climate extremes. *Plant Ecology* 215: 677–688.

Ozenda, P. G. 1985. La végétation de la chaîne alpine: dans l'espace montagnard européen. Masson, Paris, France.

Patsiou, T. S., E. Conti, N. E. Zimmermann, S. Theodoridis, and C. F. Randin. 2014. Topo-climatic microrefugia explain the persistence of a rare endemic plant in the Alps during the last 21 millennia. *Global Change Biology* 20: 2286–2300.

Pauli, H., M. Gottfried, S. Dullinger, O. Abdaladze, M. Akhalkatsi, J. L. B. Alonso, G. Coldea, et al. 2012. Recent plant diversity changes on Europe's mountain summits. *Science* 336: 353–355.

Pellizzari, E., M. Pividori, and M. Carrer. 2014. Winter precipitation effect in a mid-latitude temperature-limited environment: the case of common juniper at high elevation in the Alps. *Environmental Research Letters* 9: 104021.

Pichler, P., and W. Oberhuber. 2007. Radial growth response of coniferous forest trees in an inner Alpine environment to heat-wave in 2003. *Forest Ecology and Management* 242: 688–699.

Pornon, A., and B. Doche. 1996. Age structure and dynamics of *Rhododendron ferrugineum* L. populations in the northwestern French Alps. *Journal of Vegetation Science* 7: 265–272.

R Core Team. 2016. R: a language and environment for statistical computing. R Foundation for Statistical Computing, Vienna, Austria.

Ropars, P., E. Lévesque, and S. Boudreau. 2015. How do climate and topography influence the greening of the forest tundra ecotone in northern Québec? A dendrochronological analysis of *Betula glandulosa*. *Journal of Ecology* 103: 679–690.

Rosseel, Y. 2012. lavaan: an R package for structural equation modeling. *Journal of Statistical Software* 48: 1–36.

Russo, S., A. Dosio, R. G. Graversen, J. Sillmann, H. Carrao, M. B. Dunbar, A. Singleton, et al. 2014. Magnitude of extreme heat waves in present climate and their projection in a warming world. *Journal of Geophysical Research: Atmospheres* 119: 12500–12512.

Scherrer, D., and C. Körner. 2011. Topographically controlled thermal-habitat differentiation buffers alpine plant diversity against climate warming: Topographical control of thermal-habitat differentiation buffers alpine plant diversity. *Journal of Biogeography* 38: 406–416.

Schweingruber, F. H., A. Börner, and E.-D. Schulze. 2011. Atlas of stem anatomy in herbs, shrubs and trees. Springer, Berlin, Germany.

Shetti, R., A. Buras, M. Smiljanic, M. Hallinger, A. A. Grigoriev, and M. Wilmking. 2018. Does sex matter? Gender-specificity and its influence on site-chronologies in the common dioecious shrub *Juniperus communis*. *Dendrochronologia* 49: 118–126.

Steinbauer, M. J., J.-A. Grytnes, G. Jurasinski, A. Kulonen, J. Lenoir, H. Pauli, C. Rixen, et al. 2018. Accelerated increase in plant species richness on mountain summits is linked to warming. *Nature* 556: 231–234.

Stocker, T. F., G. K. Qin, and M. Plattner. 2013. Climate Change 2013: The physical science basis. Contribution of Working Group I to the Fifth Assessment Report of the Intergovernmental Panel on Climate Change. Cambridge University Press, Cambridge, UK.

Sturm, M., J. Schimel, G. Michaelson, J. M. Welker, S. F. Oberbauer, G. E. Liston, J. Fahnestock, and V. E. Romanovsky. 2005. Winter biological processes could help convert Arctic tundra to shrubland. *BioScience* 55: 17–26.

Touflan, P., B. Talon, and K. Walsh. 2010. Soil charcoal analysis: a reliable tool for spatially precise studies of past forest dynamics: a case study in the French southern Alps. *Holocene* 20: 45–52.

Tricart, P., and M. Lemoine. 1986. Les Schistes lustrés piémontais des Alpes Occidentales: approche stratigraphique, structurales et sédimentologique. Birkhäuser Verlag, Basel, Switzerland.

Vicente-Serrano, S. M., S. Beguería, and J. I. López-Moreno. 2010. A multiscalar drought index sensitive to global warming: the standardized precipitation evapotranspiration index. *Journal of Climate* 23: 1696–1718.

Vionnet, V., E. Brun, S. Morin, A. Boone, S. Faroux, P. Le Moigne, E. Martin, and J.-M. Willemet. 2012. The detailed snowpack scheme Crocus and its implementation in SURFEX v7.2. *Geoscientific Model Development* 5: 773–791.

Wheeler, J. A., A. J. Cortés, J. Sedlacek, S. Karrenberg, M. van Kleunen, S. Wipf, G. Hoch, et al. 2016. The snow and the willows: earlier spring snowmelt reduces performance in the low-lying alpine shrub *Salix herbacea*. *Journal of Ecology* 104: 1041–1050.

Wigley, T. M. L., K. R. Briffa, and P. D. Jones. 1984. On the average value of correlated time series, with applications in dendroclimatology and hydrometeorology. *Journal of Climate and Applied Meteorology* 23: 201–213.

Wipf, S. 2010. Phenology, growth, and fecundity of eight subarctic tundra species in response to snowmelt manipulations. *Plant Ecology* 207: 53–66.

Young, A. B., D. A. Watts, A. H. Taylor, and E. Post. 2016. Species and site differences influence climate–shrub growth responses in West Greenland. *Dendrochronologia* 37: 69–78.

Zalatan, R., and K. Gajewski. 2006. Dendrochronological potential of *Salix alaxensis* from the Kuujjua River Area, western Canadian Arctic. *Tree-Ring Research* 62: 75–82.

Zang, C., and F. Biondi. 2015. treeclim: an R package for the numerical calibration of proxy–climate relationships. *Ecography* 38: 431–436.